Textile-Integrated 3D-Printed and Embroidered Structures for Wearable Wireless Platforms

Abstract

In this paper, we present fabrication and performance evaluation of 3D-printed and embroidered textile-integrated passive ultra high frequency (UHF) radio frequency identification (RFID) platforms. The antennas were manufactured by 3D printing stretchable silver conductor directly on an elastic band. The electric and mechanical joint between the 3D-printed antennas and microchips was formed by gluing with conductive epoxy glue, by printing the antenna directly on top of the microchip structure, and by embroidering with conductive yarn. Initially, all types of fabricated RFID tags achieved read ranges of 8-9 meters. Next, the components were tested for wetting as well as for harsh cyclic strain and bending. The immersing and cyclic bending slightly effected the performance of the tags. However, they did not stop the tags from working in an acceptable way, nor did they have any permanent effect. The epoxy-glued or 3D-printed antenna-microchip interconnections were not able to endure harsh stretching. On the other hand, the tags with the embroidered antenna-microchip interconnections showed excellent wireless performance, both during and after a 100 strong stretching cycles. Thus, the novel approach of combining 3D printing and embroidery seems to be a promising way to fabricate textile-integrated wireless platforms.

Keywords

Antennas; embroidery; interconnections; passive UHF RFID; stretchable electronics; textile-integrated electronics; wearable platforms; 3D printing

Introduction

The growing interest towards wireless body area networks (WBAN), which will enable future body-centric wireless communication and sensing applications, has created a huge demand for textile-integrated electronics. The research and development work around WBAN technologies is currently very active [1-5].

One key technology in this interesting area is passive radio frequency identification (RFID) technology, which uses battery-free remotely addressable electronic tags, composed only of an antenna and a microchip [6][7]. The use of propagating electromagnetic waves in the ultra high frequency (UHF) frequency range for wirelessly powering and communicating with the passive tags enables rapid interrogation of a large number of tags. The communication with the tags is possible through various media, which means the components can e.g., be integrated into clothes. Thanks to the energy efficient mechanism of digitally modulated scattering utilized in the wireless communication between an RFID reader and tags, the data can be read from a distance of several meters. This makes the battery-free passive tags promising candidates as identification and sensing platforms as well as digital entities in future WBANs.

During actual use, these wearable wireless components have to endure many kinds on environmental stresses, such as harsh weather conditions and continuous washing [8]-[10]. Also mechanical stresses, including stretching and bending, are always involved in wearable

applications, and cause challenges for the design and manufacturing of wireless components [8][11][12]. One major reliability challenge lies in the electric and mechanical interconnections of wearable platforms [10][12].

3D direct-write dispensing is a fast and low-cost additive manufacturing method, which enables the printing of complex geometries with a high, micron resolution, accuracy. It has shown potential to be used for fabrication of conductors and antennas on textile substrates [13][14]. This 3D printing method has been recently proved to also be useful for fabrication of electric interconnections between microchips and antennas [14]. Embroidery is a simple but versatile fabrication method, with a great potential in conductor and antenna fabrication, when done using conductive yarn [5][12][15][16]. Further, embroidery has also been found to be a useful approach for embedding reliable electronic interconnections into textile materials [12][15][17]-[20]. In a word, these two techniques provide the foundation for integrating passive RFID platforms into textiles, which will be the focus of this study.

In this paper, we present the fabrication and wireless performance of textile-integrated stretchable passive UHF RFID tags, and evaluate their reliability in high moisture conditions, as well as during and after cycling bending and stretching. The tags have 3D-printed stretchable antennas, and antenna-microchip interconnections fabricated by three different ways: Firstly, by using previously commonly reported gluing with conductive silver epoxy; secondly, the antenna is 3D-printed on top of the IC fixture and thus the antenna-IC interconnection is sintered together with the antenna, this novel approach skips one process step and thus saves significant amounts of time and costs; and finally, by establishing a novel hybrid approach of 3D printing and embroidery, i.e., by sewing with conductive yarn on the printed antenna. In addition to the textile-integrated tag robustness, we evaluate the effects of the interconnection type on the tag performance and reliability.

3D printing of tag antennas

In this work, 3D direct-write dispensing was used to fabricate stretchable RFID tag antennas on a stretchable textile material, i.e., on an elastic band. A stretchable silver conductor (DuPont PE872) was selected as antenna material. The 3D printing was completed by nScrypt tabletop series 3D direct-write dispensing system; the main manufacturing parameters are defined in Table 1. The printing spacing and angle can be defined when designing the printed pattern, by a built-in software. The air pressure from a positive pressure pump is applied to the system, which pushes the ink into the main valve body, and finally through a ceramic nozzle tip. The printing system can produce a controllable ink flow, precise starts and stops, and the ability to utilize a wide range of material viscosities [21].

Table 1. 3D printing parameters.

Parameter	
Material feed pressure	16.9 Psi
Printing spacing	125 microns
Printing angle	0°
Inner diameter of tip	125 microns
Number of printed layers	1
Curing	110 °C, 15 minutes

Simple printed lines with dimension of 60 mm x 10 mm were studied first, instead of fully printed antennas, to understand the ink properties. Only one layer of ink was printed, and the lines were cured at 110 °C for 15 minutes. Fig. 1 presents the cross-section of the printed line, which shows the ink layer and the textile substrate. The conductive paste thickness

measured from different parts is 555.4 µm, 529.8 µm, and 550.9 µm. Based on these three values, the calculated average value of thickness is 545.3 µm. In addition, the ink is absorbed by the fabric substrate in some areas, which is also indicated in Fig. 1. Due to the absorption, the measured thickness in these parts is 801.3 µm.

The impact of stretching on the resistances of the printed lines was studied by stretching them from the initial length of 60 mm to 80 mm. The resistance measurements in this study were done using a Fluke 115 multimeter. The measurement probes were placed in the opposite corners of the printed lines, along longitudinal direction (60 mm).

The resistance results during strain are shown in Table 2. Then, as described in Table 3, the resistances of the printed lines were measured after 10, 20, 50, and 100 stretching cycles, where the lines were stretched from 60 mm to 80 mm and back. The frequency of the stretching cycles was 10 times / minute. The resistances were measured immediately after the stretching cycles.

The surface of a printed pattern before and during stretching is shown in Fig. 2. As can be seen, the ink layer had a good adherence to the fabric substrate before stretching. During stretching, there are some small cracks, which leads to the increase of the resistance, as presented Table 2. The increased resistances in Table 3, on the other hand, are caused by these small cracks not fully returning to their initial smooth structure immediately after strain.

Further, Table 4 shows the resistances of the lines measured immediately after the printed pattern was dipped in water for 1 minute and 10 minutes. It can be seen that wetting did not introduce any effect on the resistances of the printed patterns.

For both tests, immersing and stretching, two printed lines with the same dimension were utilized, to make sure the measurement were repeatable, and they had a similar performance in terms of resistance during the tests.

Next, the antenna design presented in Fig. 3. was printed on the stretchable textile, in order to utilize stretchable textile-integrated RFID components. The antenna is quite wide (2 cm), which reduces the impact of imperfections in the print outcome, and the length of the antenna (10 cm) is sufficient to avoid the weaknesses of electrically small antennas in the UHF frequencies from 800 MHz to 1000 MHz. Only one layer of ink was used, and also the antennas were cured at 110 °C for 15 minutes.

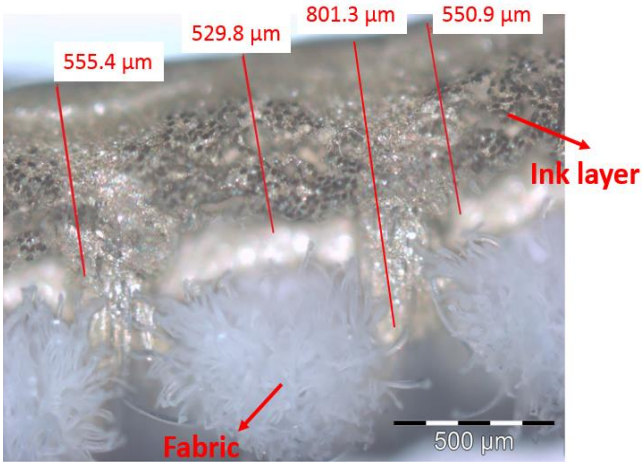

Fig. 1. Cross-section of a 3D-printed conductive line.

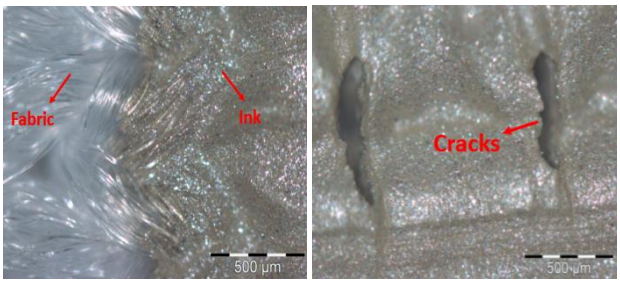

Fig. 2. Optical microscopic image of a 3D-printed line before stretching (left) and during stretching (right).

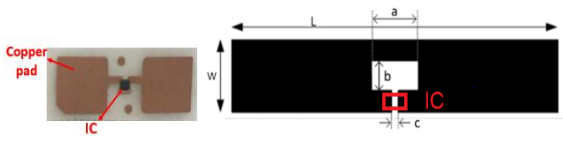

a (mm)	b (mm)	c (mm)	L (mm)	W (mm)
14.3	8.125	2	100	20

Fig. 3. A microchip strap (left) and the tag antenna structure (right).

Table 2. The resistance of the printed line during various strain positions.

Length (mm)	Resistance (Ω)
60 (initial)	0.7
70	9.2
80	21.5

Table 3. The resistance of the printed line after stretching cycles.

Stretching cycles	Resistance (Ω)
initial	0.7
10	2.3
20	5.5
50	22.4
100	66.7
After 1 week	1.9

Table 4. The resistance of the printed line in high humidity conditions.

Time in water (min)	Resistance (Ω)
initial	0.7
1	0.7
10	0.7

IC attachment methods

The used microchip, i.e., integrated circuit (IC) was NXP UCODE G2iL series RFID IC, provided by the manufacturer in a strap patterned from copper on a plastic film. The IC strap structure is shown in Fig. 3.

Three different methods were studied for the antenna-microchip interconnection: The first method was a commonly used way, where the IC is attached on top of the printed and cured antenna with conductive silver epoxy (Circuit Works CW2400). This method has been used, e.g., in [10][12][16]. It is proved that this epoxy glue shows good conductivity and establishes a well-working electric interconnection between antenna and IC. However, some challenges have been reported, such as reliability problems under mechanical stress and continuous washing [10][12].

In the second method, the antenna was deposited on top of the IC strap pads, and thus the antenna-IC interconnection was cured together with the antenna. Before printing, a reference point on the fabric substrate needs to be set using the built-in software of the 3D printer, in order to determine the position of the antenna. Then, IC strap is placed on the exact position on the substrate, and the antenna is printed on the substrate and on the IC strap copper pads. This recently invented 3D-printing approach skips one process step, and thus saves significant amounts of time and costs. This type of 3D-printed interconnection has showed suitable electric performance in recent studies, where graphene ink [14] and non-stretchable silver ink [13] have been used to fabricate RFID tags. However, no reliability evaluations have been reported.

In the third method, embroidery technique was utilized for attaching the IC on the printed antenna pattern. The IC strap copper pads were embroidered on the 3D-printed tag antenna using Husqvarna Viking embroidery machine and conductive yarn (Shieldex multifilament thread 110f34 dtex 2-ply HC). The DC linear resistivity of the thread is 500 ± 100 Ω/m, and the diameter is approximately 0.16 mm. We attached the IC strap copper pads to the 3D-printed antennas by embroidering a cross over them with conductive yarn, as shown in Fig 4. This type of attachment has been previously utilized with embroidered and electro-textile antennas [10][16].

To the best of our knowledge, this paper is the first presentation of combining embroidered and 3D-printed structures on textile-integrated RFID platforms.

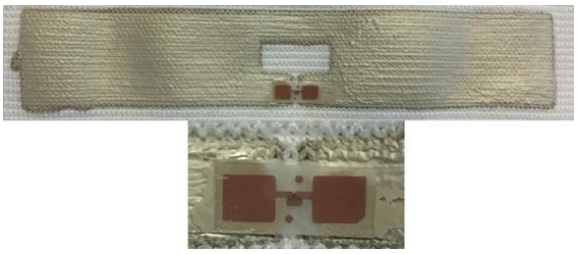

(a)

(b)

(c)

Fig. 4. Ready RFID tags and magnifications of the antenna-IC interconnections: (a) epoxy-glued joint, (b) 3D-printed joint, (c) embroidered joint.

For each tag type, two samples were fabricated to also evaluate the reproducibility. All three types of ready 3D-printed tags with different IC attachment methods and corresponding magnifications of the antenna-IC interconnections are shown in Fig. 4.

Wireless measurements

The tags were tested wirelessly using Voyantic Tagformance measurement system [22], which includes an RFID reader with an adjustable transmission frequency (0.8…1 GHz) and output power (up to 30 dBm), and provides the recording of the backscattered signal strength (down to −80 dBm) from the tag under test.

All the measurements were conducted with the tested tag suspended on a foam fixture in an anechoic chamber. The measurements were obtained from a fixed angle between the reader antenna and the tag, in order to achieve optimized performance and high read range. The angle was 0 degrees, which means the longer side of the antenna, where the IC was attached, was directly facing the reader antenna.

During the test, we recorded the lowest continuous-wave transmission power (threshold power: P_{th}) at which the tag remained responsive. Here we defined P_{th} as the lowest power at which a valid 16-bit random number from the tag is received as a response to the query command in ISO 18000-6C communication standard. In addition, the wireless channel from the reader antenna to the location of the tested tag was characterized using a system reference tag with known properties. As detailed in [23], this enabled the measurement device to estimate the attainable read range of the tag (d_{Tag}) from

$$d_{Tag} = \frac{\lambda}{4\pi}\sqrt{\frac{EIRP}{\Lambda}\frac{P_{th}{}^{*}}{P_{th}}},$$

where P_{th} is the measured threshold power of the tag, Λ is a known constant describing the sensitivity of the system reference tag, P_{th*} is the measured threshold power of the system reference tag, and EIRP is the emission limit of an RFID reader, given as equivalent isotropic radiated power. All results correspond to EIRP = 3.28 W, which is the emission limit in European countries.

Based on the calibration data provided by the manufacturer of the measurement system, we have estimated that the maximum variability in d_{Tag} due to variability in the system reference tag (Λ) and the output power meter of the reader (P_{th} and P_{th*}) is less than 5 % throughout the studied frequency range.

Measurement results

Fig. 5 shows the attainable read ranges of all types of fabricated tags. As can be seen, all these tags initially showed similar wireless performance and both "same type of tags" showed similar performance. The peak read ranges of the tags with epoxy-glued joint, 3D-printed joint, and embroidered joint were 8.8 meters, 9.6 meters, and 8.1 meters, respectively. These results are very promising when compared to earlier reported RFID tag results: The performance is similar or superior to 3D-printed silver and copper RFID tags, respectively [13], and significantly superior to 3D-printed graphene RFID tags [14] on textile substrates. Further, none of these previously reported 3D-printed RFID components has been stretchable.

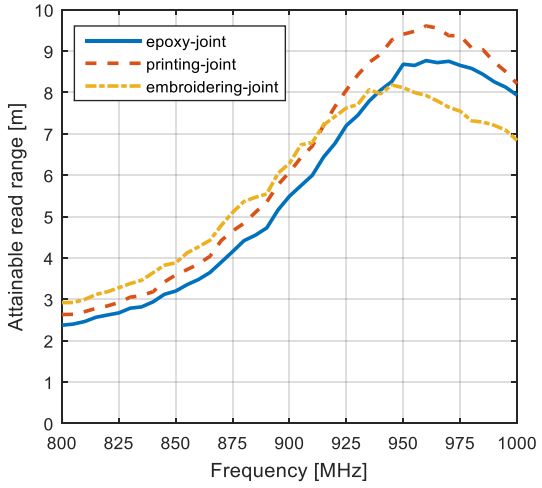

Fig. 5. Attainable read ranges of all types of stretchable tags in original state.

Next, three types of reliability evaluation tests, including an immersing test, a bending test, and a stretching test, were performed.

A. Immersing test

First, the effects of very high humidity and wetting on the tag performance were investigated. During the test, the tags were placed in tap water (pH = 6.5-7), as shown in Fig. 6, and wirelessly measured before the test and immediately after 1 minute in water. The tags were then left in room conditions to dry, and were measured again after 1 hour, and after 1 day. The wireless performance of the tags during and after the test are shown in Fig. 7.

Based on the measurement results, the read ranges of all types of tags decrease after 1 minute in water. The absorbed moisture affects the dielectric constant and loss tangent of the fabric substrate, which affects the performance of the antenna, as well as the antenna-IC impedance matching, and thus the wireless performance of the tags. After drying for one hour in room conditions, the read ranges of all types of tags have increased close to normal, but there is still a significant shift in the peak frequency range, caused by the absorbed moisture. After 1 day, when the tags are dry again, the wireless responses of all types of tags have returned to the initial performance. Thus, the harsh test did not have a permanent effect on the performance of these tags.

B. Bending test

In the bending test, the tags were bent over a 30 mm thick structure in Y-direction, as shown in Fig. 6. The wireless performance was measured at different steps: before bending, when bent, and in a non-bended state after up to 100 bending cycles. The frequency of the bending cycles was 10 times / minute. Fig. 8 shows the read ranges of all types of tags when testing the bending performance. As can be seen, the read ranges of all types of tags decrease about 2 meters during bending, but when measured in the non-bended state, the performance of these tags is stable even after a 100 times of bending.

C. Stretching test

In the stretching test, the performance of the tags was studied by stretching them from the initial length of 100 mm to 105 mm, 110 mm, and 115 mm. The stretching was done by attaching the tags to the foam structure with tape. The components were measured during each elongation. Based on the results, the tags with epoxy-glued IC attachment and 3D-printed IC attachment were not stretchable, since the antenna-IC interconnections of these tags were easily broken. See Fig. 9 for broken IC attachments. The attainable read ranges of the tags with embroidered antenna-IC interconnections under incremental strains from 0 % to 15 % are presented in Fig. 10 (a). In addition, Fig. 10 (b) shows the attainable read ranges in a non-stretched state after 20, 50, and 100 stretching cycles, where the tags were stretched from 100 mm to 115 mm each time. The frequency of the stretching cycles was 10 times / minute. After all stretching cycles, the tags recovered in room conditions for 5 days, and the performance was measured again.

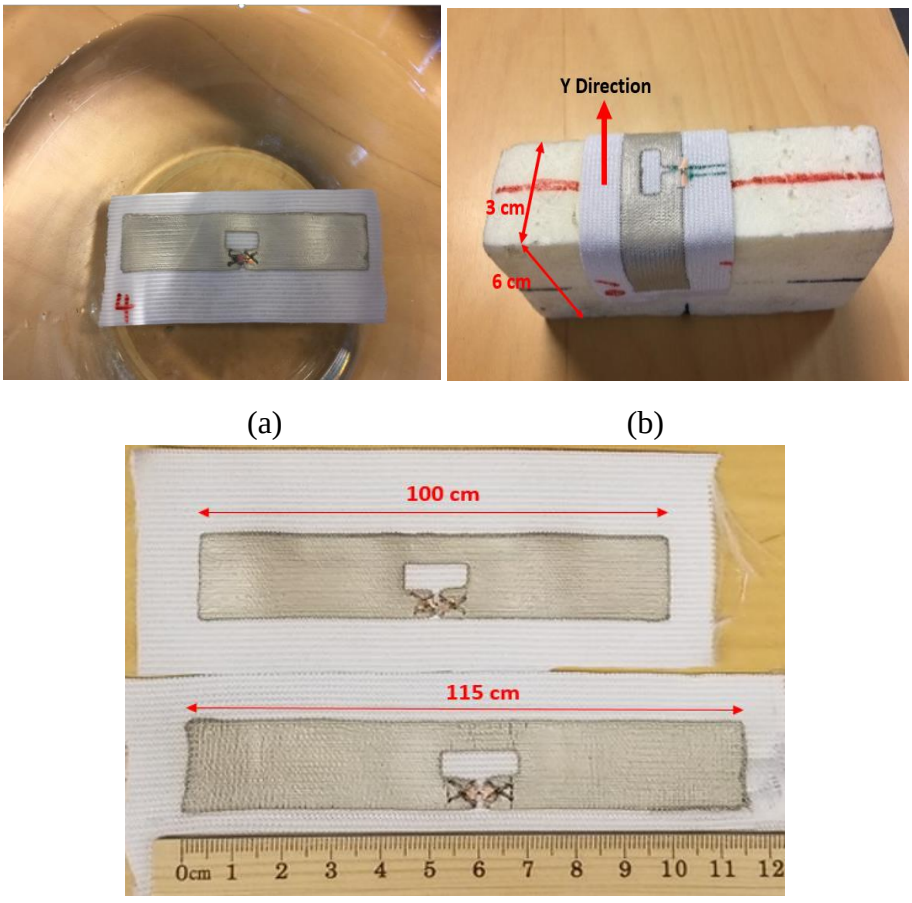

(a) (b)

(c)

Fig. 6. Reliability evaluations: (a) immersing test, (b) bending test, (c) stretching test.

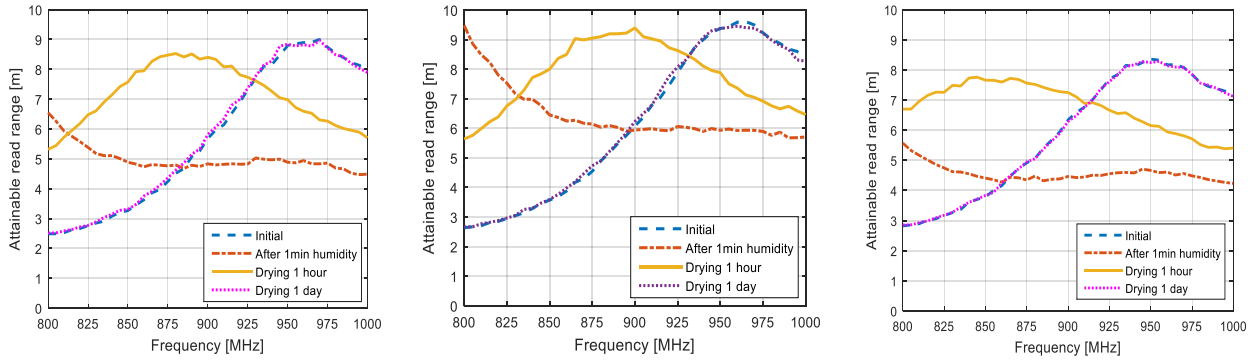

(a) (b) (c)

Fig. 7. Attainable read ranges of tags in the immersing reliability test: (a) tag with a glued antenna-IC joint, (b) tag with a 3D-printed antenna-IC joint, (c) tag with an embroidered antenna-IC joint.

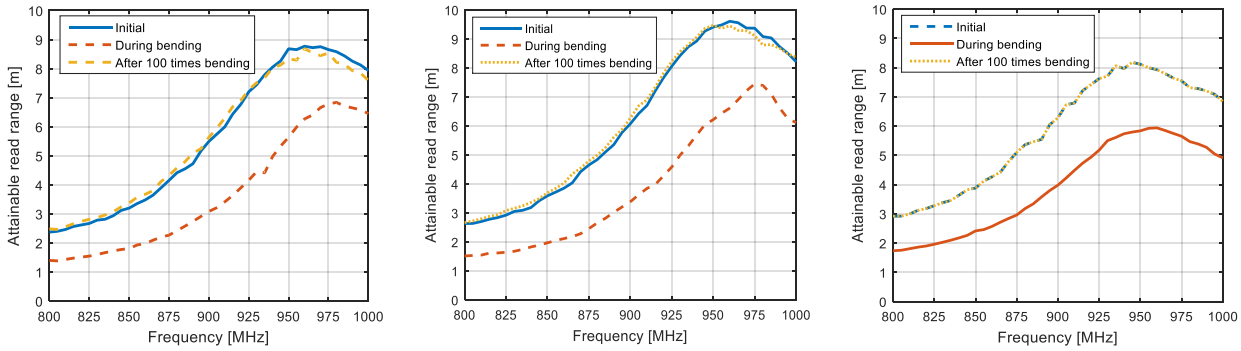

(a) (b) (c)

Fig. 8. Attainable read ranges of tags in bending reliability test: (a) tag with a glued antenna-IC joint, (b) tag with a 3D-printed antenna-IC joint, (c) tag with an embroidered antenna-IC joint.

The results in Fig. 10 (a) show that the tags with embroidered antenna-IC joints experienced a slight downward shift in the frequency of the peak read range when stretched increasingly. It is noticeable that the peak read range value was only slightly effected by the harsh strain, and the tags showed excellent read ranges of over 6 meters throughout the global UHF frequency band, even when stretched from 100 mm to 115 mm.

Moreover, as shown in Fig. 10 (b), after a 100 stretching cycles (stretched from 100 mm to 115 mm each time), the peak read range was still around 7 meters. It can be seen that the reduction in the performance of the non-stretched state tag also declined with the number of stretching cycles. After recovered 5 days in room conditions, the read range returned to 8 meters, which is only 0.8 meters less than the initial performance. It should also be noted a read range of 7 meters is still a very good result, especially since the tag is readable throughout the global UHF RFID band (860-960 MHz).

All the reliability evaluation tests and their results are summarized in Table 5.

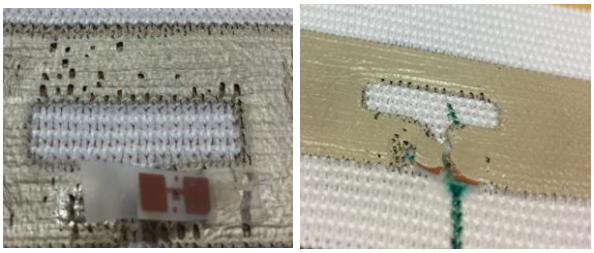

Fig. 9. Broken antenna-IC interconnections of epoxy-glued joint (left) and 3D-printed joint (right).

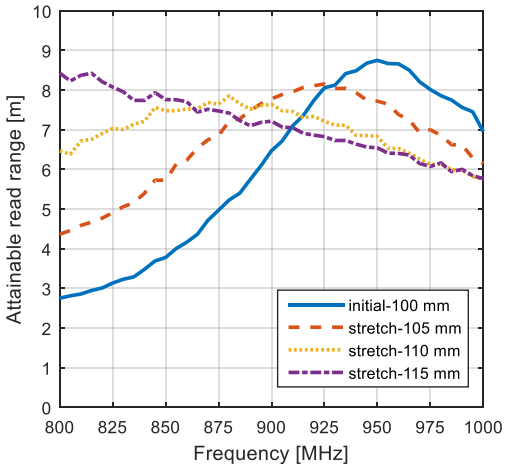

(a)

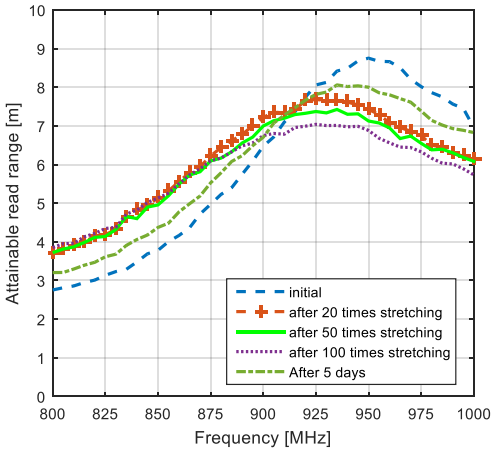

(b)

Fig. 10. Attainable read ranges of a tag with an embroidered antenna-IC joint: (a) during various elongations, (b) after multiple stretching cycles (stretched from 100 mm to 115 mm each time).

Table 5. Reliability evaluation results.

IC attachment method	Peak read range	Immersing test	Bending test	Stretching test
Epoxy-glued	8.8 m	good	good	fail
3D-printed	9.6 m	good	good	fail
Embroidered	8.2 m	good	good	good

Conclusions

In this paper, the possibility of 3D printing on a stretchable textile material using stretchable silver conductor was studied for RFID tag antenna fabrication. For microchip attachment, conductive epoxy glue, 3D printing, and embroidery were used, in order to find the most reliable methods to embed wireless platforms into textiles.

Initially, the tags with 3D-printed antenna-IC joints achieved the longest read ranges, which were around 0.8 meters and 1.6 meters better than the tags with epoxy-glued and embroidered joints, respectively.

Wetting and cyclic bending did not stop the tags from working in a suitable way, and they did not have any permanent effect on the tags' wireless performance. The results of the immersing test show the great potential of our wearable tags in a high humidity environment. These tags could work near a sweating body and even when dipped in water. Moreover, the bending test results indicate that the tags could be bended repeatedly while maintaining a stable performance, which is very important when integrating these platforms into clothing. The tags with embroidered antenna-IC attachment on a 3D-printed antenna showed the best reliability in continuous strain, as they were the only ones withstanding harsh stretching. Moving to stretchable antennas and interconnections will lead the way for practical integration of electronics into clothing. A combination of 3D printing and embroidery is a promising fabrication approach for solving the current reliability challenges in RFID antenna-IC interconnections and for taking the next steps in establishment of textile-integrated identification and sensing platforms. The next phase is to test the washing reliability of these fabricated tags, by combining mechanical stresses and moisture in a washing machine. This also means that suitable coating methods and materials need to be studied. In the future, we also plan to replace the stretchable silver conductor with a carbon-based stretchable conductor, which will offer a lower cost.

References

1. Van-Daele P, Moerman I and Demeester P. Wireless body area networks: status and opportunities. In: General Assembly and Scientific Symposium (URSI GASS), Beijing, China, 16-23 August 2014.
2. Zheng YL, Ding XR, Poon CCY, Lo BPL, Zhang H, Zhou XL and Zhang YT.

Unobtrusive sensing and wearable devices for health informatics. IEEE Trans. Biomed. Eng. 2014; 61.5: 1538–1554.
3. Kennedy T, Fink P, Chu A, Champagne N, Gregory Y, Lin G and Khayat M. Body-worn E-textile antennas: the good, the low-mass, and the conformal. IEEE Transactions on Antennas and Propagation 2009; 57.4: 910–918.
4. Manzari S, Occhiuzzi C and Marrocco G. Feasibility of body-centric systems using passive textile RFID tags. IEEE Antennas and Propagation Magazine 2012; 54.4: 49-62.
5. Kaufmann T, Fumeaux IM and Fumeaux C. Comparison of fabric and embroidered dipole antennas. In: European Conference on Antennas and Propagation, Gothenburg, Sweden, 8-12 April 2013, pp. 325–3255.
6. Want R. An introduction to RFID technology. IEEE Pervasive Computing 2006; 5: 25–33.
7. Dobkin D, The RF in RFID: passive UHF RFID in practice. Newnes-Elsevier, 2008.
8. Patron D, et al. On the use of knitted antennas and inductively coupled RFID tags for wearable applications. IEEE Trans. Biomed. Circuits Syst. 2016; 10.6: 1047-1057.
9. Nayak R, Singh A, Padhye R and Wang L, RFID in textile and clothing manufacturing: technology and challenges. Fashion and Textiles 2015; 2.1: 9.
10. Wang S, Chong N, Virkki J, Björninen T, Sydänheimo L and Ukkonen L. Towards washable electro-textile UHF RFID tags: reliability study of epoxy-coated copper fabric antennas. International Journal of Antennas and Propagation 2015.
11. Shao S, Kiourti A, Burkholder R, Volakis JL. Flexible and stretchable UHF RFID tag antennas for automotive tire sensing. In: Proc. Eur. Conf. Antennas Propag. (EuCAP), The Hague, Netherlands, 6-11 April 2014, pp. 2908-2910.
12. Chen X, Liu A, Wei Z, Ukkonen L and Virkki J. Experimental study on strain reliability of embroidered passive UHF RFID textile tag antennas and interconnections. Journal of Engineering 2017.
13. Björninen T, Virkki J, Sydänheimo L and Ukkonen L. Possibilities of 3D direct write dispensing for textile UHF RFID tag manufacturing. In: IEEE International Symposium on Antennas and Propagation & USNC/URSI National Radio Science Meeting, Vancouver, BC, Canada, 19-24 July 2015, IEEE, pp. 1316–1317.
14. He H, Akbari M, Sydänheimo L, Ukkonen L and Virkki J. 3D-Printed Graphene antennas and interconnections for textile RFID tags: fabrication and reliability towards humidity. International Journal of Antennas and Propagation 2017.
15. Ginestet G, Brechet N, Torres T, Moradi E, Ukkonen L, Bjorninen T and Virkki J. Embroidered antenna-microchip interconnections in passive UHF RFID textile tags, IEEE Antennas and Wireless Propagation Letters 2017; 16: 1205-1208.
16. Moradi E, Bjorninen T, Ukkonen L and Rahmat-Samii Y, Effects of sewing pattern on the performance of embroidered dipole-type RFID tag antennas, IEEE Antennas and Wireless Propagation Letters 2012; 11: 1482–1485.
17. Berglund ME, Duval J, Simon C and Dunne LE. Surface-mount component attachment for e-textiles. In: Proceedings of ACM International Symposium on Wearable Computers, Osaka, Japan, 7-11 September 2015, p. 65-66.
18. Post ER, Orth M, Russo PR and Gershenfeld N. E-broidery: design and fabrication of textile-based computing. IBM Syst. J. 2000; 39: 840–860.
19. Linz T, Kallmayer C, Aschenbrenner R and Reichl H. Embroidering electrical interconnects with conductive yarn for the integration of flexible electronic modules into fabric. In: Wearable Computers, Ninth IEEE International Symposium on, Osaka, Japan, 18-21 Octorber 2005, pp. 86-89.
20. Linz T, Vieroth R, Dils C, Koch M, Braun T, Becker KF, Kallmayer C and Hong SM. Embroidered interconnections and encapsulation for electronics in textiles for

wearable electronics applications. Adv. Sci. Technol. 2008; 60: 85–94.
21. Nscrypt USA, Smart Pump. http://www.nscrypt.com/wp-content/uploads/2017/02/2016-SmartPump-Gen2.pdf, accessed on Apr. 2017.
22. Voyantic Ltd. Tagformance. http://www.voyantic.com/tagformance, accessed on Apr. 2017.
23. Virkki J, Björninen T, Merilampi S, Sydänheimo L and Ukkonen L. The effects of recurrent stretching on the performance of electro-textile and screen-printed ultra-high-frequency radio-frequency identification tags. Text. Res. J. 2015; 85: 294–301.